REMARKS

Claims 1-4, 6-10, 12, 14-21, 48-50 and 52-61 are pending. All of the pending claims stand rejected. Applicants respectfully request reconsideration of the rejections based on the following comments.

Applicants thank the Examiner for the courtesy extended to their undersigned representative in a phone interview on August 31, 2006. In the phone interview the remaining issues were discussed, and the context of the previously submitted section 132 Declaration was reviewed in view of the remaining rejections. Applicants' representative and the Examiner discussed options for advancing the application.

Rejection Under 35 U.S.C. § 112

The Examiner rejected claims 1-4, 6-10, 12-21 and 48-61 under 35 U.S.C. § 112, second paragraph as being indefinite. For conciseness, Applicants incorporate by reference their arguments from the Responses of March 29, 2005, August 15, 2005 and March 14, 2006, and focus here on the Examiner's response to those arguments. The Examiner asserts that "less than" and "greater than" describe "definite maximum and minimum" values that are contradicted by the term "about." With all due respect, Applicants have searched the PTO web site and have found since 1976 there have been **53,976** patents issued with the phrase "less than about" in their claims. Many of these have been issued recently. A copy of the first two pages of the search is attached. Similarly, **28,519** patents have issued since 1976 with the phrase "greater than about" in their claims. Either there are countless incompetent patent examiners, which Applicants do not believe is true, or the phrase is not inherently indefinite. Applicants have argued case law and the perspective of an ordinary person of skill in the art. The Examiner has failed to assert why in the present context that the phrases are unclear. Thus, with all due respect, the Examiner

has failed to establish *prima facie* indefiniteness. Applicants respectfully request withdrawal of the rejection of claims 1-4, 6-10, 12-21 and 48-61 under 35 U.S.C. § 112, second paragraph as being indefinite.

Rejection Over Kamauchi et al. and Manev

The Examiner rejected claims 1-4, 6, 7, 10, 12, 14-17, 19-21, 48-50, 52, 53 and 55-61 under 35 U.S.C. § 103(a) as being unpatentable over U.S. Patent 5,538,814 to Kamauchi et al. (the Kamauchi patent) in view of U.S. Patent 5,789,115 to Manev (the Manev patent). Applicants previously submitted Declaration evidence that the grinding approach suggested in the Kamauchi patent was not suitable for producing the uniform materials claimed in the pending claims above. The Examiner cited the Manev patent for teaching that "the mean particle size and the particle size distribution are two of the basic properties characterizing the positive electrode intercalation materials." Applicants assert that the Manev patent does not make up for the deficiencies of the Kamauchi patent, that the combined teachings of the references do not enable the production of the claimed materials and that the Manev patent teaches away from the claimed invention. Thus, the combined teachings of the cited references do not render Applicants' invention *prima facie* obvious. Applicants respectfully request reconsideration of the rejection based on the following comments.

With respect to the Manev patent, this patent explicitly teaches away from its combination with the Kamauchi patent. In particular, the Manev patent teaches that the particles should not necessarily be too small. See column 1, lines 50-67. In fact, all of the preferred materials taught in the Manev patent have a mean particle size greater than 1 micron, see for example, column 3, lines 53-61. Thus, Manev teaches away from Applicants' claimed particle sizes.

While a reference is prior art for all that it teaches, references along with the knowledge of a person of ordinary skill in the art must be enabling to place the invention in the hands of the public. In re Paulsen, 31 USPQ2d 1671, 1675 (Fed. Cir. 1994). See also In re Donohue, 226 USPQ 619, 621 (Fed. Cir. 1985). "The consistent criterion for determination of obviousness is whether the prior art would have suggested to one of ordinary skill in the art that this process should be carried out and would have a reasonable likelihood success, viewed in light of the prior art." Micro Chemical Inc. v. Great Plains Chemical Co., 41 USPQ2d 1238, 1245 (Fed. Cir. 1997)(quoting In Re Dow Chemical Co., 5 USPQ2d 1529, 1531 (Fed. Cir. 1988)).

The proposition is well established that the cited art only renders a composition of matter or apparatus unpatentable to the extent that the cited art enables the disputed claims, in other words, if the cited art provides a means of obtaining the claimed composition or apparatus.

> To the extent that anyone may draw an inference from the Von Bramer case that the mere printed conception or the mere printed contemplation which constitutes the designation of a 'compound' is sufficient to show that such a compound is old, regardless of whether the compound is involved in a 35 U.S.C. 102 or 35 U.S.C. 103 rejection, we totally disagree. ... We think, rather, that the true test of any prior art relied upon to show or suggest that a chemical compound is old, is whether the prior art is such as to place the disclosed 'compound' in the possession of the public. In re Brown, 141 USPQ 245, 248-49 (CCPA 1964)(emphasis in original)(citations omitted).

On page 7 of the office action, it is stated that one "of ordinary skill in the art, based on Kamauchi and Manev, to prepare or select particles of preferred sizes without grinding or by pulverizing or filtering the material." However, at column 2, lines 17-20, the Manev patent notes that for their materials of interest "grinding ... is not a desirable method of reducing the mean particle size and particle size distribution ... ." But grinding is the approach taught in Kamauchi for reducing particle size. With all due respect, while Manev indicates that grinding is a non-preferred optional way to prepare the material, they teach a synthesis technique that directly

forms the lithium manganese oxide powders with the desired particle sizes. See, for example, the examples in Manev. There is no teaching whatsoever that their techniques can be used to make phosphates nor would one expect these techniques to be successful to make phosphates. Kamauchi only teaches grinding to make submicron particles. Kamauchi does not exemplify the generation of submicron particles. Applicants have demonstrated that grinding of phosphates made by techniques in the Kamauchi and Goodenough patents does not produce particles close to the claimed particle uniformity. Due to problems of agglomeration as well as inherent distributions of pore sizes, filtration cannot be used to achieve high levels of submicron particle uniformity. Due to these multiple deficiencies in the teachings in the art, the Examiner has not provided a teaching of how the public had possession of the claimed invention directed to highly uniform submicron inorganic phosphate particles prior to the filing date.

Due to the experience of the present inventors with respect to the high rate capability of submicron and in particular nanoscale electrode materials, the inventors took on the development of the presently claimed phosphate nanoparticles. See, U.S. 6,503,646. To accomplish their objectives, the present inventors had to develop techniques to synthesize inorganic materials with complex anions using laser pyrolysis. These were very significant developments that allowed for the production of the presently claimed materials. Since the time that the present inventors performed this work, the research community has confirmed that the inherent low rate capabilities of these materials can be overcome through the use of small, submicron particle size to reduce the distance required for Li^+ transport. See, Striebel article attached at page A669, right column first full paragraph. Additionally, bulk lithium iron phosphate needs a carbon coating to overcome its very low electrical conductivity (about 10^{-9} to 10^{-10} S/cm), which causes considerable ohmic drop within the electrode at high rates. It has recently been validated that small, uniform lithium iron phosphate powders have improved performance as a result of their improved rate capability in an unrelated effort by a French government laboratory. See the

attached article to Delacourt et al. and Striebel article at page A669, right column, first full paragraph. These results are consistent with Applicants previous experience that uniform submicron particles have improved rate performance.

In summary, the cited references do not point to Applicants' claimed invention involving submicron uniform particles, the combined teachings of the cited references do not provide a reasonable expectation of success and the claimed materials have unexpectedly improved performance, as demonstrated with similar material recently synthesized. Therefore, the Examiner has fallen far short of establishing a *prima facie* showing of obviousness. Since there is no *prima facie* obviousness over the cited references, Applicants respectfully request withdrawal of the rejection of claims 1-4, 6, 7, 10, 12, 14-17, 19-21, 48-50, 52, 53 and 55-61 under 35 U.S.C. § 103(a) as being unpatentable over the Kamauchi patent in view of the Manev patent.

Rejection Over Kamauchi et al. Manev et al. and Goodenough et al.

The Examiner rejected claims 8, 9 and 18 under 35 U.S.C. § 103(a) as being unpatentable over U.S. Patent 5,910,382 to Goodenough et al. (the Goodenough patent) in view of the Kamauchi patent and the Manev patent as applied to the corresponding independent claims. The deficiencies of the Kamauchi patent and the Manev patent are described in detail above. The Goodenough patent does not make up for the deficiencies of the Kamauchi patent and the Manev patent described in detail above. In particular, the Goodenough patent does not teach or suggest anything about particle size or uniformity. Therefore, the combined teachings of the Kamauchi patent, the Manev patent and the Goodenough patent do not render claims 8, 9 and 18 *prima facie* obvious. Applicants respectfully request withdrawal of the rejection of claims 8, 9 and 18 under 35 U.S.C. § 103(a) as being unpatentable over the Goodenough patent in view of the Kamauchi patent and the Manev patent as applied to the corresponding independent claims.

Rejection Over Bodiger et al. and Bi et al.

The Examiner rejected claims 54-56, 58, 59 and 61 under 35 U.S.C. § 103(a) as being unpatentable over U.S. Patent 5,849,827 to Bodiger et al. (the Bodiger patent) in view of U.S. Patent 5,952,125 to Bi et al. (the Bi patent). The Examiner admitted that the Bodiger patent has many shortcomings. The Examiner cited the Bi patent for teaching uniform materials. With all due respect, Applicants respectfully assert that the Examiner has fallen far short of establishing *prima facie* obviousness. Applicants respectfully request reconsideration of the rejections based on the following comments.

"To establish a prima facie case of obviousness, three basic criteria must be met. First, there must be some suggestion or motivation, either in the references themselves or in the knowledge generally available to one of ordinary skill in the art, to modify the reference or to combine reference teachings. Second, there must be a reasonable expectation of success. Finally, the prior art reference (or references when combined) must teach or suggest all the claim limitations. The teaching or suggestion to make the claimed combination and reasonable expectation of success must both be found in the prior art, and not based on applicant's disclosure." MPEP § 2142 (citing In re Vaeck, 947 F.2d 488, 20 USPQ2d 1438 (Fed. Cir. 1991)).

As an initial matter, Applicants would like to clear up some confusion that may have inadvertently propagated over rejections based on the Bodiger patent. In particular, claim 54 depends from claim 21, which has a significantly different scope from the other claims. With respect to claim 54, neither the Bodiger patent nor the Bi patent teach or suggest lithium metal phosphates. This alone should be dispositive with respect to this claim. Claims 55, 56, 58, 59 and 61 do not have this feature.

With all due respect, the rejection generally has many levels of deficiencies. For example, neither reference teaches how to make nanoscale phosphates. In particular, the Bi

patent does not teach how to make inorganic particles with complex anions. Thus, while the Bi patent teaches laser pyrolysis, it does not teach formation of metal phosphate powders. Thus, the combined teachings of the references do not place the claimed materials in the hands of the public. The only phosphate compound described at all in either reference is aluminum phosphate. Applicants could not find any description of metal phosphates generally given that phosphorous itself is not a metal.

The Examiner stated that "It would be obvious to one of ordinary skill in the art at the time that the invention was made to prepare a mixture with essentially no particle with a diameter greater than about 3 or 5 times the average particle size OR that at least about 95 percent of the particles have a diameter greater than about 40 percent and less than about 160 percent of the average diameter, as one of ordinary skill in the art would recognize that when a desired average diameter is disclosed in the prior art, choosing particles close to that diameter would be desirable for the function described in the reference." With all due respect, this does not follow at all from the knowledge in the art. The Bodiger reference teaches only average particle sizes. The reference says nothing at all about the desired uniformity of the materials. The Bodiger patent describes a surprising and not understood reduction in burn times due to the inclusion of the inorganic particles. See column 1, lines 51-56. For all that is known, a broad distribution in particle sizes is needed to obtain this behavior. The Examiner's broad statement to the contrary is certainly not a suggestion in the art that flame retardants would benefit from more uniform particles. Furthermore, the reference certainly does not suggest how such uniform materials could be obtained. Thus, there is simply no teaching of all of the claim elements, and the Bodiger patent does not provide a reasonable expectation of success.

The Bi patent does not teach how to make inorganic phosphate particles or any other particles with complex, multi-atom, anions. Thus, the Bi patent does not place the presently claimed uniform phosphate particles in the hands of the public. In this regard, the Bi patent does

not make up for the deficiencies of the Bodiger patent. Also, the Bi patent does not describe the desirability of uniform nanoscale phosphate particles.

In summary, the Bodiger patent and the Bi patent alone or combined fail to teach, motivate or provide a reasonable expectation of success with respect to the claimed particle size uniformity. With all due respect, the Examiner has fallen short of establishing *prima facie* obviousness of Applicants' claimed invention over the Bodiger patent in view of the Bi patent. Applicants respectfully request withdrawal of the rejection of claims 54-56, 58, 59 and 61 under 35 U.S.C. § 103(a) as being unpatentable over the Bodiger patent in view of the Bi patent.

CONCLUSIONS

In view of the foregoing, it is submitted that this application is in condition for allowance. Favorable consideration and prompt allowance of the application are respectfully requested.

The Examiner is invited to telephone the undersigned if the Examiner believes it would be useful to advance prosecution.

Respectfully submitted,

Peter S. Dardi

Peter S. Dardi, Ph.D.
Registration No. 39,650

Customer No. 62274
Dardi & Associates, PLLC
Suite 2000, U.S. Bank Plaza
220 South 6th Street
Minneapolis, Minnesota 55402
Telephone: (404) 949-5730

USPTO Patent Full-Text and Image Database

Home | Quick | Advanced | Pat Num | Help

Next List | Bottom | View Cart

Searching US Patent Collection...

Results of Search in US Patent Collection db for:
ACLM/"less than about": 53976 patents.
Hits 1 through 50 out of 53976

Next 50 Hits

Jump To

Refine Search ACLM/"less than about"

	PAT. NO.	Title
1	7,107,287	Method, system and storage medium for automated independent technical review
2	7,107,144	Non-intrusive traffic monitoring system
3	7,107,113	Method for optimizing a supply-consumption operation
4	7,106,936	Homogenizer for collimated light controlled high angle scatter
5	7,106,917	Resonant optical modulators
6	7,106,893	Method and apparatus for segmenting small structures in images
7	7,106,777	Phase-change heat exchanger
8	7,106,604	System and method for reducing transfer function ripple in a logarithmic RMS-to-DC converter
9	7,106,554	Perpendicular magnetic writer with magnetic potential control shield
10	7,106,519	Tunable micro-lens arrays
11	7,106,517	Display optical films
12	7,106,501	Fiber amplifier with suppression of amplified spontaneous emission
13	7,106,412	Lithographic apparatus comprising a gas flushing system
14	7,105,996	Electron gun for color CRT
15	7,105,983	Electrical contact technology and methodology for the manufacture of large-diameter electrical slip rings
16	7,105,928	Copper wiring with high temperature superconductor (HTS) layer
17	7,105,925	Differential planarization
18	7,105,908	SRAM cell having stepped boundary regions and methods of fabrication
19	7,105,811	Control system and apparatus for use with laser excitation of ionization

20 7,105,762 Rocker switch and actuator therefor
21 7,105,610 Thin-layer-covered golf ball with improved velocity
22 7,105,609 Alpha-olefin/propylene copolymers and their use
23 7,105,601 Adhesive resin with high damping properties and method of manufacture thereof
24 7,105,497 Methods of optimizing drug therapeutic efficacy for treatment of immune-mediated gastrointestinal disorders
25 7,105,466 Siliceous clay slurry
26 7,105,452 Method of planarizing a semiconductor substrate with an etching chemistry
27 7,105,434 Advanced seed layery for metallic interconnects
28 7,105,303 Antibodies to hepatitis C virus asialoglycoproteins
29 7,105,266 Polymers containing oxygen and sulfur alicyclic units and photoresist compositions comprising same
30 7,105,252 Carbon coated battery electrodes
31 7,105,240 Perpendicular media with improved corrosion performance
32 7,105,215 Ink jet recording element
33 7,105,201 Versatile processes for preparing and using novel composite particles in powder coating compositions
34 7,105,197 Process for preparing intermediate moisture vegetables
35 7,105,190 Products comprising an isothiocyanate preservative system and methods of their use
36 7,105,185 Kavalactone profile
37 7,105,174 Multiple-delayed release anti-neoplastic product, use and formulation thereof
38 7,105,108 Graphite intercalation and exfoliation process
39 7,105,107 Use of nonmicroporous support for syngas catalyst
40 7,105,086 Storm drain capture and containment device
41 7,105,055 In situ growth of oxide and silicon layers
42 7,105,051 High quality colloidal nanocrystals and methods of preparing the same in non-coordinating solvents
43 7,105,050 Method for the production of low defect density silicon
44 7,105,036 Drift eliminator, light trap, and method of forming same
45 7,104,823 Enhanced separable connector with thermoplastic member and related methods
46 7,104,822 Electrical connector including silicone elastomeric material and associated methods
47 7,104,463 Base isolated nebulizing device and methods
48 7,104,336 Method for fighting fire in confined areas using nitrogen expanded foam
49 7,104,333 Dry pipe valve for fire protection sprinkler system
50 7,104,319 In situ thermal processing of a heavy oil diatomite formation

Next List | Top | View Cart
Home | Quick | Advanced | Pat Num | Help

USPTO Patent Full-Text and Image Database

Home | Quick | Advanced | Pat Num | Help

Next List | Bottom | View Cart

Searching US Patent Collection...

Results of Search in US Patent Collection db for:
ACLM/"greater than about": 28519 patents.
Hits 1 through 50 out of 28519

Next 50 Hits

Jump To

Refine Search ACLM/"greater than about"

	PAT. NO.	Title
1	7,107,287	Method, system and storage medium for automated independent technical review
2	7,107,144	Non-intrusive traffic monitoring system
3	7,106,917	Resonant optical modulators
4	7,106,777	Phase-change heat exchanger
5	7,106,656	Sonar system and process
6	7,106,501	Fiber amplifier with suppression of amplified spontaneous emission
7	7,106,432	Surface inspection system and method for using photo detector array to detect defects in inspection surface
8	7,106,183	Rearview camera and sensor system for vehicles
9	7,106,088	Method of predicting high-k semiconductor device lifetime
10	7,105,996	Electron gun for color CRT
11	7,105,989	Plasma lamp and method
12	7,105,908	SRAM cell having stepped boundary regions and methods of fabrication
13	7,105,610	Thin-layer-covered golf ball with improved velocity
14	7,105,607	Tear resistant gels, composites, and articles
15	7,105,601	Adhesive resin with high damping properties and method of manufacture thereof
16	7,105,588	Screen printable hydrogel for medical applications
17	7,105,584	Dual-cure silicone compounds exhibiting elastomeric properties
18	7,105,497	Methods of optimizing drug therapeutic efficacy for treatment of immune-mediated gastrointestinal disorders
19	7,105,466	Siliceous clay slurry

20 7,105,440 Self-forming metal silicide gate for CMOS devices
21 7,105,434 Advanced seed layery for metallic interconnects
22 7,105,361 Method of etching a magnetic material
23 7,105,311 Systems and methods for detection of analytes in biological fluids
24 7,105,201 Versatile processes for preparing and using novel composite particles in powder coating compositions
25 7,105,185 Kavalactone profile
26 7,105,114 Briquetting of lime based products with carbon based additives
27 7,105,105 Deicing/anti-icing fluids
28 7,105,082 Composition and method for electrodeposition of metal on a work piece
29 7,105,051 High quality colloidal nanocrystals and methods of preparing the same in non-coordinating solvents
30 7,104,823 Enhanced separable connector with thermoplastic member and related methods
31 7,104,822 Electrical connector including silicone elastomeric material and associated methods
32 7,104,720 Traffic noise barrier system
33 7,104,702 Field installable optical fiber connector
34 7,104,676 Signaling assembly
35 7,104,265 Filter containing a metal phthalocyanine and a polycationic polymer
36 7,104,238 Apparatus and method for lessening the accumulation of high boiling fraction from fuel in intake valves of combustion engines
37 7,103,251 Dispersion flattened NZDSF fiber
38 7,103,137 Radiation scanning of objects for contraband
39 7,103,083 Optimized graphite electrode pin configuration
40 7,103,079 Pulsed quantum dot laser system with low jitter
41 7,102,862 Electrostatic discharge protection circuit
42 7,102,854 Transducing head with reduced side writing
43 7,102,824 Optical element for efficient sensing at large angles of incidence
44 7,102,705 Backlight assembly and liquid crystal display device having the same
45 7,102,350 Shielding apparatus for magnetic resonance imaging
46 7,102,235 Conformal lining layers for damascene metallization
47 7,102,172 LED luminaire
48 7,102,052 Activated vapor treatment for neutralizing warfare agents
49 7,101,888 Oral liquid tolterodine composition
50 7,101,862 Hemostatic compositions and methods for controlling bleeding

Next List | Top | View Cart
Home | Quick | Advanced | Pat Num | Help

A352 *Electrochemical and Solid-State Letters*, 9 (7) A352-A355 (2006)
1099-0062/2006/9(7)/A352/4/$20.00 © The Electrochemical Society

Size Effects on Carbon-Free $LiFePO_4$ Powders

The Key to Superior Energy Density

C. Delacourt,[a,*] P. Poizot,[a] S. Levasseur,[b] and C. Masquelier[a,z]

[a]*Laboratoire de Réactivité et de Chimie des Solides, UMR CNRS 6007, Université de Picardie Jules Verne, Amiens Cedex 9, France*
[b]*UMICORE Research and Development, B-2250 Olen, Belgium*

C-free $LiFePO_4$ crystalline powders were prepared by a synthesis method based on direct precipitation under atmospheric pressure. The particle size distribution is extremely narrow, centered on ca. 140 nm. A soft thermal treatment, typically at 500°C for 3 h under slight reducing conditions was shown to be necessary to obtain satisfactory electrochemical Li^+ deinsertion/insertion properties. This thermal treatment does not lead to grain growth or sintering of the particles, and does not alter the surface of the particles. The electrochemical performances of the powders obtained by this synthesis method are excellent, in terms of specific capacity (147 mAh g^{-1} at 5C-rate) as well as in terms of cyclability (no significant capacity fade after more than 400 cycles), without the need of carbon coating.
 [DOI: 10.1149/1.2201987] All rights reserved.

Manuscript submitted February 10, 2006; revised manuscript received March 20, 2006. Available electronically May 12, 2006.

Olivine-type $LiFePO_4$, namely, triphylite, was first proposed by Padhi et al. in 1997 to be used as a positive electrode material for Li-ion batteries.[1] Li^+ deinsertion/insertion of this compound occurs at a potential value of ca. 3.45 V vs Li^+/Li with a high theoretical specific capacity of 171 mAh g^{-1}. The main drawback of this cheap and nontoxic material is its low gravimetric density besides a poor electrical conductivity which limits the Li^+ deinsertion/insertion rates, and hence the practical specific capacity. To overcome this problem, several chemical routes so as to produce carbon coatings at the surface of $LiFePO_4$ particles were proposed.[2] Besides increasing the overall conductivity of the material through an electronic percolating network around the particles, one generally agrees that such coating also prevents particle growth and sintering during annealing treatments.[3-6]

The presence of carbon has a dramatic impact though on the tap density of the powder: it is reduced by 2 when only 2 wt % carbon is present in the composite material, which gives energy densities only half of those of standard materials such as $LiCoO_2$.[7] Moreover, a recent comparative electrochemical study and kinetic modeling of $LiFePO_4$ powders from different sources concluded that the average particle size of the materials, as well as their distribution (namely, the psd), must be narrowed in order to obtain an ideal material.[8]

AC and dc conductivity measurements of C-free $LiFePO_4$ dense pellets suggest that carbon coating is far from being the only route to explore for producing a more efficient $LiFePO_4$ electrode. Li^+ conductivity is indeed likely to be in the same order of magnitude or even lower than the electronic one.[9] A recent DFT contribution of Maxisch et al. confirms our experimental data, as a transport mechanism involving ($Li_{Li}^{\cdot}$, c_{Fe}') and ($\square_{Li}'$, $h_{Fe}^{\cdot}$) exciton-like quasi particles (in $FePO_4$ and $LiFePO_4$, respectively) is envisaged.[10] Limitations appear then to be both ionic and electronic which strengthen the importance of tailoring as small particles as possible so as to shorten both electronic and ionic paths within the particles.

Along that line, Chimie douce is a well-known method to prepare materials having controlled particle size with narrow size distributions. Among the numerous recent contributions on the precipitation of iron-based nanocompounds, one may quote nano-Fe_3O_4 and nano-Fe_2O_3,[11,12] nanoparticles of amorphous hydrated iron phosphates of formula $FePO_4 \cdot nH_2O$.[13] Regarding $LiFePO_4$, soft chemistry has been restricted so far to the precipitation under hydrothermal conditions.[14-22] Tajimi and Nuspl demonstated first that carbon coating was not any longer essential for providing good electrochemical activity: through the use of surfactants such as PEG, carbon-free $LiFePO_4$ particles ranged between 0.5 and 1.5 μm with a specific capacity of 140 mAh g^{-1} at a current density of 0.5 mA cm^{-2}.[20] Nuspl et al. reported on a carbon-free powder with a narrow particle size distribution (average in the 400 to 600 nm range) that could deliver 114 mAh g^{-1} at 8C rate.[17-19]

Experimental

Based on our recent findings on the direct precipitation of crystalline $LiMnPO_4$ with particle size around 100 to 150 nm, under atmospheric conditions,[23] we used a similar approach for the synthesis of carbon-free $LiFePO_4$ particles at low temperature under atmospheric pressure.[24] To this end, we first undertook a detailed thermodynamic study of the $Li^+/Fe(II)$/phosphate/H_2O system following our extensive previous studies on the precipitation of $FePO_4 \cdot 2H_2O$ allotropes.[25] Precipitation of $LiFePO_4$ may occur at an optimal pH value close to neutrality as plotted in the solubility-pH diagram shown in Fig. 1. A mixture of 0.1 mol L^{-1} of Fe(II) sulfate ($FeSO_4 \cdot 7H_2O$, Sigma Aldrich) and 0.1 mol L^{-1} H_3PO_4 (Baker) was neutralized to this average pH value by slowly adding 0.3 mol L^{-1} of LiOH ($LiOH \cdot H_2O$, Alfa Aesar), leading to a green mixture which was subsequently kept under refluxing conditions for ca. 16 h under magnetic stirring. The green-grayish precipitate thus obtained was then recovered by centrifugation, washed several times with distilled water and acetone and finally dried in an oven at 50°C for one day (Fig. 2). For electrochemical measurements, the precipitate was previously annealed for 3 h at 500°C under a N_2/H_2 gas flow in order to fully dehydrate the material and reduce the possible Fe(III)-containing impurities.

X-ray diffraction (XRD) experiments were performed on a Philips PW 1710 diffractometer (θ-2θ, Cu Kα radiation, back monochromator). Powders' morphology was observed by scanning electron microscopy (SEM) by means of a Philips FEG XL-30 and by transmission electron microscopy (TEM) and high-resolution TEM (HRTEM) by using a FEI Technai F20 S-Twin. Particle size distribution (psd) was determined from image analysis of SEM pictures of the $LiFePO_4$ powder. Electrochemical lithium deinsertion/insertion tests were performed either in Swagelok-type cells or in coin cells, which were both assembled in an argon-filled dry box. The negative electrode was a disk of lithium metal foil. A Whatman GF/D borosilicate glass fiber sheet, soaked with a 1 M $LiPF_6$ salt dissolved in 1:1 EC/DMC solution (Merck, LP30), was placed between the two electrodes. The positive electrodes simply consisted in a mixture of the C-free $LiFePO_4$ obtained from the precipitation and ketjen black carbon (EC-600 JD, Akzo Nobel), by means of a mortar and a pestle. When used in a Swagelok, the positive electrode

* Electrochemical Society Student Member.
z E-mail: christian.masquelier@u-picardie.fr

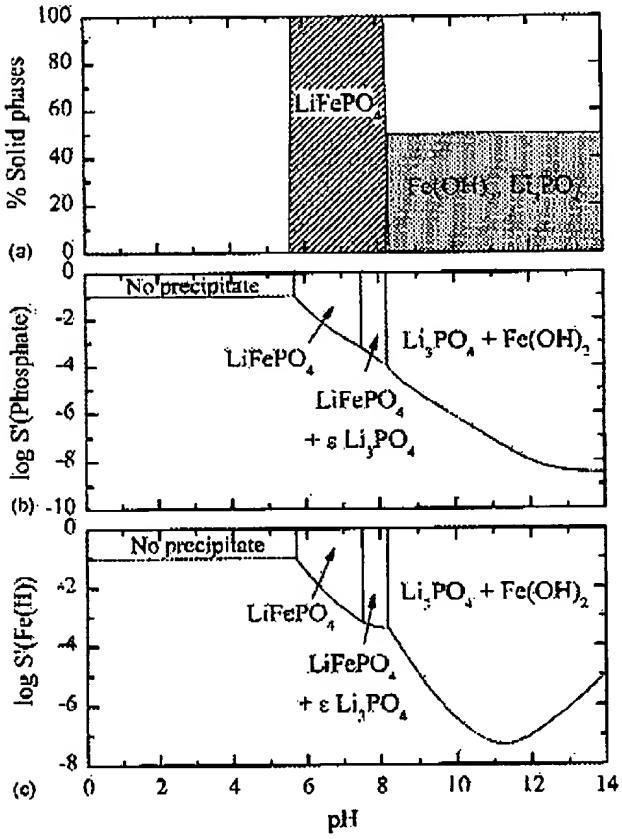

Figure 1. (a) Distribution diagram of solid compounds in equilibrium with the solution (molar ratio). (b) Solubility diagram of phosphate. (c) Solubility diagram of Fe(II). Conditions: $[Fe(II)]_{ini} = [Phosphate]_{ini} = 0.1$ M. $[Li^+] = 1$ M, an hypothetical pK_s value of 12 was chosen for $LiFePO_4$.

material thus obtained was directly led onto the current collector (typical loading of ~ 14 mg for 1.3 cm^2 current collector area). For coin cells, a slurry of the electrode material and *N*-methylpyrrolidone (NMP) was made and deposited onto the current collector. The electrodes were left for at least 3 h in an oven at 100°C in order to fully evaporate the NMP. The typical loading in this case was comprised between 2 and 5 mg (for 1.9 cm^2 current collector area). Lithium deinsertion/insertion was monitored either with MacPile or VMP cycling/data recording systems (Biologic SA, Claix, France), operating in galvanostatic mode.

Results and Discussion

The XRD pattern of the precipitate obtained for 16 h aging under refluxing conditions is given in Fig. 2. It was entirely indexed in the space group *Pnma* reported for $LiFePO_4$ (ICSD no. 200155) with lattice constants $a = 10.294(2)$ Å, $b = 5.974(1)$ Å, and $c = 4.694(1)$ Å, i.e., smaller than usually encountered for $LiFePO_4$ prepared through more classic ceramic routes. We do not know yet what is at the exact origin of such behavior. Unlike $LiMnPO_4$,[23] the nucleation and growth of the olivine-type phase $LiFePO_4$ occurs very quickly as crystalline samples were obtained after as small as 15 min under refluxing conditions. The nucleation step is thus likely to be predominant over the growth, which leads to very small particle size comprised between 100 and 200 nm, as illustrated in the inset of Fig. 2.

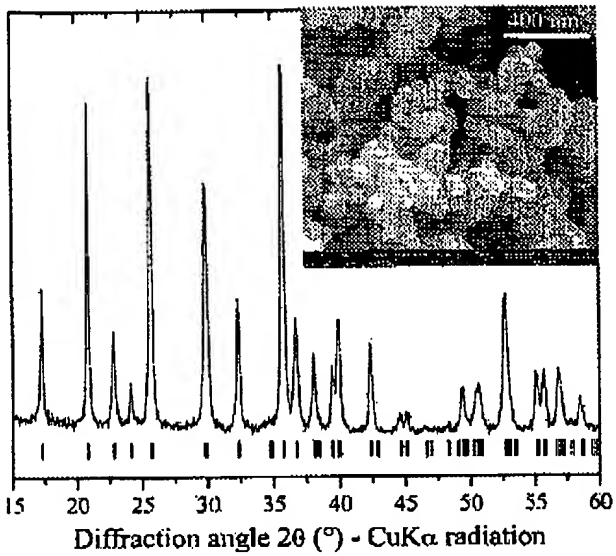

Figure 2. XRD diagram of the as-obtained precipitate after 16 h of reaction under refluxing conditions. Inset: SEM image of the particles, having size comprised between 100 and 200 nm.

Prior to perform electrochemical characterizations of the $LiFePO_4$ powder, a heat-treatment under reducing conditions (typically a N_2/10% H_2 gas flow) was ensured so as to reduce the small amount of Fe(III) together with the removal of parasitic "OH" groups through water departure. Indeed, Mössbauer spectroscopy revealed that the pristine $LiFePO_4$ powders may contain up to 15–20 atom % of Fe(III). The presence of O-H groups was attested by Fourier transform (FTIR) measurements: a weak absorption band was detected at ~3270 cm^{-1} and was related to O-H bond stretching into the amorphous $LiFePO_4(OH)$ phase, from a comparison with the FTIR spectrum of crystalline $LiFePO_4(OH)$ (Tavorite, ICDD no. 41-1376) (not shown here). This also suggests that slight amounts of amorphous $LiFePO_4(OH)$ composition are present within the powder, which is concordant with the presence of Fe(III). Figures 3a and b are SEM and TEM micrographs of a $LiFePO_4$ sample heat-treated at 500°C for 3 h under N_2/10% H_2 gas flow. Note that the temperature and the dwell time of the thermal treatment are significantly reduced compared to a ceramic synthesis process. Coarsening of $LiFePO_4$ particles is hence significantly reduced, and the average particle size remains in the range of 100–200 nm. Note, however, that the particle morphology has changed during the thermal treatment, from parallelepipeds for the as-made precipitate to spheres for the annealed powders. From SEM analyses, the particle size distribution (psd) could be determined (Fig. 3c). The d50 value is ~140 nm, while the relative span, defined as (d90-d10)/d50, is about 0.50. The psd is much narrower and shifted toward smaller values than that reported by Nuspl et al. for $LiFePO_4$ hydrothermally synthesized.[17,18]

Surface reactivity is generally enhanced for divided powders, especially during thermal treatments. To identify the possible existence of parasitic phases such as iron phosphides at the surface of the heat-treated $LiFePO_4$ powders, HRTEM observations coupled with EDX analyses in STEM mode across $LiFePO_4$ particles were carried out (not shown here). The absence of any amorphous layer at the surface of the particles together with the constancy of the Fe/P atomic ratio from the particle core to the surface clearly accounts for the absence of an iron phosphide layer around the particles. This conclusion was strengthened by ac conductivity measurements on dense sintered pellets of the material which show that the electrical

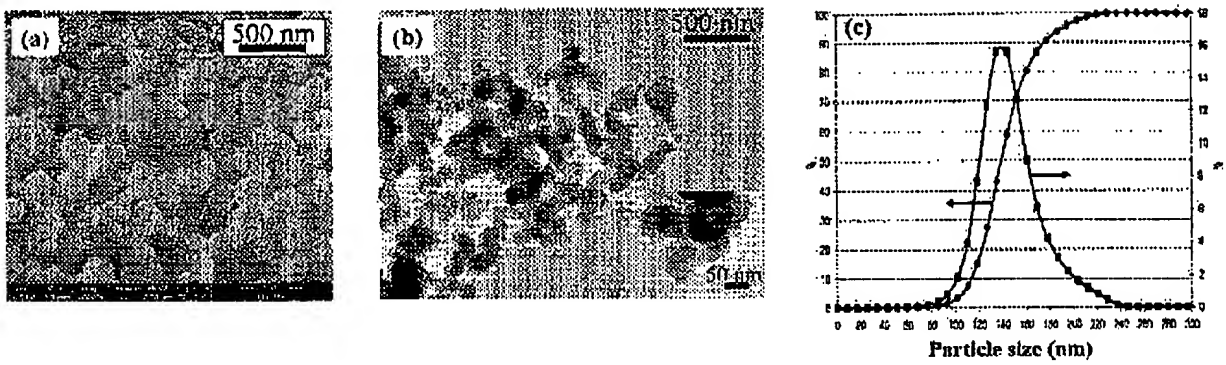

Figure 3. (a) SEM, (b) TEM, and (c) volumetric particle size distribution (obtained from image analysis of SEM images) of the C-free $LiFePO_4$ powder obtained after a heat-treatment at 500°C under N_2/10% H_2 atmosphere for 3 h.

conductivity value of the bulk is comparable to that reported in Ref. 9 for pure $LiFePO_4$, prepared through a ceramic route (not shown here).

As shown in Fig. 4, Li^+ deinsertion/insertion of the $LiFePO_4$ powder mixed with only 5 wt % of ketjen black carbon proceeds with an extremely small polarization, even under high current rates (C/2 during discharge), leading to a high reversible specific capacity of ca. 145 mAh g^{-1}. This excellent performance is mostly due to the lowering of the particle size, and hence we wish to stress that carbon coating is no longer required for such a divided material. Note also that no significant capacity fade was observed, even after more than 400 charge/discharge cycles: this may be due to the observed fact that $LiFePO_4$ particles are highly monodisperse (very narrow psd centered on 140 nm) leading to an homogeneous current distribution within the electrode. Figure 5 shows signature curves obtained by varying several parameters, such as the amount of carbon in the positive electrode, as well as the type of positive electrode and cell configuration used. At low charge/discharge rates, an increase of the carbon amount from 5 to 16.7% leads to a constant increase of the specific capacity of ~15 mAh g^{-1}, whatever the C-rate used. For higher charge/discharge rates (typically >1 C for cells made with powders), the influence of the carbon amount becomes more important. Even at 5 C rate, discharge specific capacities as high as 135 and 147 mAh g^{-1} are obtained for $LiFePO_4$ electrodes made from NMP-based slurries, and containing 5 and 16.7 wt % ketjen black carbon, respectively.

Conclusion

A soft chemistry method allowed the preparation of C-free $LiFePO_4$ particles in the range 100–200 nm, with a very narrow particle size distribution. This material, after a heat-treatment under slightly reducing conditions, exhibits very satisfactory electrochemical properties in terms of specific capacity and capacity retention upon cycling. These properties are directly linked to the small particle size, which lowers both ionic and electronic transport within the particles. The performances reported here, in terms of specific capacity related to the active material, are identical or slightly higher than those reported for C-coated $LiFePO_4$.[3,5,26] They are therefore superior in terms of energy density due to the absence of C-coating. To conclude, besides being very attractive on a practical aspect, $LiFePO_4$–type electrodes bring us new insights about the importance of size effects on the electrochemical activity. By transposing the same concepts to more insulating materials such as $LiMnPO_4$, one would expect that a huge decrease of the particle size should be the key point for an enhancement of its electrochemical activity.

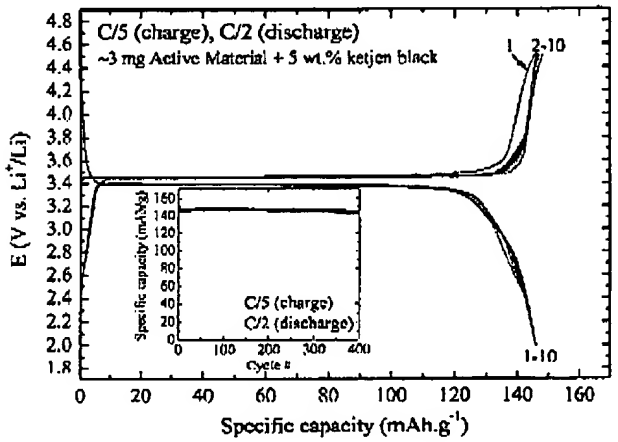

Figure 4. Galvanostatic charge/discharge profiles at 20°C of an electrode composed of C-free $LiFePO_4$ (heat-treated powder) mixed with 5 wt % of ketjen black carbon. The charge rate (1 e^- per formula unit exchanged in 5 h) is lower that than of discharge (1 e^- per formula unit exchanged in 2 h). Inset: Specific capacity retention of the active material.

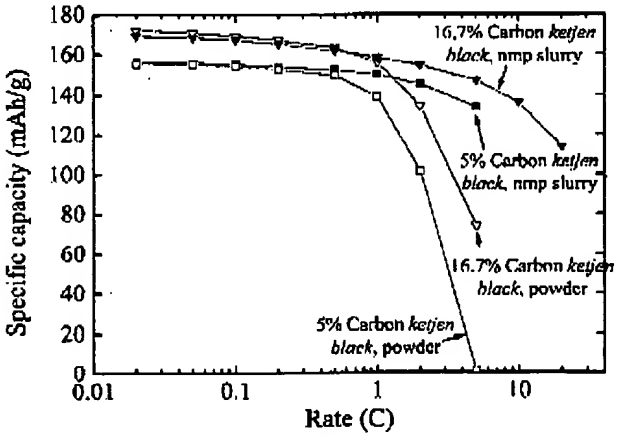

Figure 5. Evolution of the specific capacities relative to the active material as a function of C-rate, at 20°C. Electrodes made from NMP slurries are composed of ~3 mg of active material + ketjen black carbon and are cycled in coin cells. Electrodes directly made from powders of AM + ketjen black carbon are loaded with ~14 mg and are cycled in Swagelok-type cells.

Acknowledgments

The authors gratefully acknowledge J.-M. Tarascon and P. Gibot for fruitful discussions, as well as L. Laffont for TEM observations.

Université de Picardie Jules Verne assisted in meeting the publication costs of this article.

References

1. A. K. Padhi, K. S. Nanjundaswamy, and J. B. Goodenough, *J. Electrochem. Soc.*, **144**, 1188 (1997).
2. N. Ravet, J. B. Goodenough, S. Besner, M. Simoneau, P. Hovington, and M. Armand, Abstract 127, The Electrochemical Society Meeting Abstracts, Vol. 99-2, Honolulu, HI, Oct 17–22, 1999.
3. H. Huang, S. C. Yin, and L. F. Nazar, *Electrochem. Solid-State Lett.*, **4**, A170 (2001).
4. A. Audemer, C. Wurm, M. Morcrette, S. Gwizdala, and C. Masquelier, World Pat. WO 2004/001881 A2 (2004).
5. K. Dominko, J. M. Goupil, M. Bele, M. Gaberscek, M. Remskar, D. Hanzel, and J. Jamnik, *J. Electrochem. Soc.*, **152**, A607 (2005).
6. K.-F. Hsu, S.-Y. Tsay, and B.-J. Hwang, *J. Mater. Chem.*, **14**, 2690 (2004).
7. Z. Chen and J. R. Dahn, *J. Electrochem. Soc.*, **149**, A1184 (2002).
8. K. Striebel, J. Shim, V. Srinivasan, and J. Newman, *J. Electrochem. Soc.*, **152**, A664 (2005).
9. C. Delacourt, L. Laffont, R. Bouchet, C. Wurm, J.-B. Leriche, M. Morcrette, J.-M. Tarascon, and C. Masquelier, *J. Electrochem. Soc.*, **152**, A913 (2005).
10. T. Maxisch, F. Zhou, and G. Ceder, *Phys. Rev. B*, **73**, 104301 (2006).
11. J. P. Jolivet, M. Henry, J. Livage, and E. Bescher, *Metal Oxide Chemistry and Synthesis*, 1, Wiley & Sons, New York (2000).
12. D. Larcher, C. Masquelier, D. Bonnin, Y. Chabre, V. Masson, J.-B. Leriche, and J.-M. Tarascon, *J. Electrochem. Soc.*, **150**, A133 (2003).
13. X. Wang, X. Yang, H. Zheng, J. Jin, and Z. Zhang, *J. Cryst. Growth*, **274**, 214 (2005).
14. S. Yang, P. Y. Zavalij, and M. S. Whittingham, *Electrochem. Commun.*, **3**, 505 (2001).
15. S. Franger, F. Le Cras, C. Bourbon, and H. Rouault, *Electrochem. Solid State Lett.*, **5**, A231 (2002).
16. S. Franger, F. L. Cras, C. Bourbon, and H. Rouault, *J. Power Sources*, **119–121**, 252 (2003).
17. G. Nuspl, Paper 293 presented at IMLB 12 Meeting, 2004.
18. G. Nuspl, Paper 63 presented at IBA 2004, 2004.
19. G. Nuspl, L. Wimmer, and M. Eisgruber, World Pat. WO 2005/051840 A1 (2005).
20. S. Tajimi, Y. Ikeda, K. Uematsu, K. Toda, and M. Sato, *Solid State Ionics*, **175**, 287 (2004).
21. J. Lee and A. S. Teja, *J. Supercrit. Fluids*, **35**, 83 (2005).
22. C. Masquelier, D. Delacourt, C. Wurm, L. Laffont, and M. Morcrette, Paper 19 presented at IMLB XII, 2004.
23. C. Delacourt, P. Poizot, M. Morcrette, J. M. Tarascon, and C. Masquelier, *Chem. Mater.*, **16**, 93 (2004).
24. C. Delacourt, P. Poizot, and C. Masquelier, Eur. Pat. EP05291406.6 (2006).
25. C. Delacourt, C. Wurm, P. Reule, M. Morcrette, and C. Masquelier, *Solid State Ionics*, **173**, 113 (2004).
26. A. Yamada, S. C. Chung, and K. Hinokuma, *J. Electrochem. Soc.*, **148**, A224 (2001).

Journal of The Electrochemical Society, 152 (4) A664-A670 (2005)
0013-4651/2005/152(4)/A664/7/$7.00 © The Electrochemical Society, Inc.

Comparison of $LiFePO_4$ from Different Sources

Kathryn Striebel,*,z Joongpyo Shim,* Venkat Srinivasan,* and John Newman**

Lawrence Berkeley National Laboratory, Environmental Energy Technologies Division, Berkeley, California 94720, USA

The lithium iron phosphate chemistry is plagued by poor conductivity and slow diffusion in the solid phase. To alleviate these problems, various research groups have adopted different strategies, including decreasing the particle sizes, increasing the carbon content, and adding dopants. In this study, we obtained $LiFePO_4$ powders and/or electrodes from six different sources and used a combined model-experimental approach to compare the performance. Samples ranged from 0.4 to 15% "*in situ*" carbon. In addition, particle sizes varied by as much as an order of magnitude between samples. The study detailed in this manuscript allows us to provide insight into the relative importance of the conductivity of the samples compared to the particle size, the impact of having a distribution in particle sizes, and ideas for making materials to maximize the power capability of this chemistry.

Manuscript submitted June 25, 2004; revised manuscript received September 14, 2004.
Available electronically February 10, 2005.

Lithium iron phosphate ($LiFePO_4$) is a promising candidate for low-cost lithium batteries because it has a high theoretical capacity (170 mAh/g), excellent stability during cycling, and prospects for a safer cell compared with $LiCoO_2$.[1] The major drawback with this material has been that it has low electronic conductivity, on the order of 10^{-9} S/cm.[2] This renders it difficult to prepare cathodes capable of operating at high rates. Significant research has recently been focused on the incorporation of conductive carbon into the active material powders[3-5] or the doping of the $LiFePO_4$ structure to improve its electronic conductivity.[2,6] Our group has been studying the carbon-coated $LiFePO_4$ invented at Hydro-Quebec[3] and now supplied by PhosTech (Montreal, Canada) in pouch cells prepared with natural graphite anodes and either liquid[7] or gel electrolytes.[8] Huang *et al.* reported the preparation of $LiFePO_4$ in a carbon gel matrix where the active material is dispersed in a carbon prepared from a resorcinol gel.[4] More recently, other labs are reporting excellent results from carbon-coated $LiFePO_4$ made by other techniques such as gel-coating[9] and a carbothermal technique.[10] In addition to having low electronic conductivity, lithium and/or electron diffusion in the active material has been reported to be slow, with considerable loss in utilization with increasing current.[11]

Because of the low electronic conductivity of the active material, $LiFePO_4$, the performance of a $LiFePO_4$ cathode depends on the amount of carbon in the structure, either *in situ* (*i.e.*, either formed during the preparation of the active material or formed intentionally by adding, *e.g.*, sugar solution followed by carbonization) or mixed in with the binder. However, Doeff *et al.* also found that the relative quality of the *in situ* carbon on the $LiFePO_4$ particles plays a major role in cathode performance.[12] The quality of the carbon, resulting from the addition of different organic precursors, was compared by measuring the sp^2/sp^3 character of the carbon in the $LiFePO_4$ after firing, by Raman spectroscopy.

In another approach to the problem, Chiang *et al.* claimed that doping (substituting) of part of the Li in the structure for Nb, Zr, or Mg resulted in an increase in the electronic conductivities by eight orders of magnitude.[2] However, there have recently been some challenges to those findings.[13] The improvement of the electronic conductivity of an active-material powder is difficult to measure because most preparations involve organic precursors that result in residual carbon. In addition, the conductivity measurement requires dense pellets that, in turn, require higher temperatures (for sintering) than what is used to prepare cathode-active powders. This increases the risk for converting part of the $LiFePO_4$ into other (highly conductive) phases such as Fe_2P.[14]

There are clearly several approaches to the preparation of a low electronic conductivity active material, such as $LiFePO_4$, into a high-performance cathode. The relative intrinsic conductivity as well as the location and quality of the added or *in situ* carbon play a role. In addition, poor solid-phase transport means that the utilization of the active material is a strong function of the particle size. Together, these factors lead to a strong dependence of cathode performance on the loading and thickness of the electrode. This dependence on loading makes it difficult to compare the merits of different preparation techniques for $LiFePO_4$. In this work, we prepared cathodes from many sources of $LiFePO_4$. The performance at different rates was measured in half-cells, and the inevitable differences in cathode design were normalized through the use of a mathematical model of the discharge process in the $LiFePO_4$ cathode.

The model is based on the one developed previously by Doyle *et al.* in that it incorporates charge and mass balance in the porous electrode and reaction at the interface.[15] Whereas the previous models have described the solid-phase phenomenon using intercalation behavior (diffusion in spherical coordinates), the present model describes the phase change that is known to occur in $LiFePO_4$ using the "shrinking core" approach[16] in keeping with X-ray diffraction (XRD) evidence of the existence of two phases.[11]

Experimental

$LiFePO_4$ powders with varying amounts of *in situ* carbon (carbon resulting from the phosphate preparation) were used as received from the Institute of Chemistry (Ljubljana, Slovenia), Hydro-Quebec (HQ) (Quebec, Canada), the University of Waterloo (Waterloo, Canada), and the State University of New York (SUNY, Binghamton, NY). The $LiFePO_4$ powders were combined with carbon black (Shawinigan) and/or graphite (SFG-6) and mixed into a slurry with poly(vinylidene fluoride) (PVdF, Kureha)/*N*-methyl pyrrolidone. Slurries were cast with a knife-edge coater on carbon-coated Al current collectors, prepared in-house from a very thin coating of PVdF-bonded Shawinigan black. These electrodes were made in a near-identical manner to minimize the impact of electrode construction. In addition, premade cathodes were received from the Massachusetts Institute of Technology (MIT) and the Lawrence Berkeley National Laboratory (LBNL) Materials Science Division. The MIT cathode was prepared from 1% Zr-doped $LiFePO_4$,[2] and the LBNL cathode contained $LiFePO_4$ prepared with the sol-gel technique with the addition of pyromellitic acid to the precursor mix.[12] The compositions of each electrode (*i.e.*, active material, carbon and/or graphite and binder content) as well as thickness and loading were known. Several of these parameters are listed in Table I. The electrodes were tested in identical Swagelok cells with the same electrode area (1 cm^2) and a spring-loaded current collection piston so as to maintain similar compression during testing. However, as the two premade cathodes were not constructed in an identical manner to the rest, changing the fabrication technique could yield differences in the results from the ones reported in this paper. In other words, the

* Electrochemical Society Active Member.
** Electrochemical Society Fellow.
z E-mail: kastriebel@lbl.gov

Table I. Properties of $LiFePO_4$ powders and cathodes.

Source	*In situ* carbon (%)	Particle size (nm)	Crystallite size (nm)	Active loading (mg/cm²)	Total carbon (%)	Binder (PVdF) (%)	Electrode thickness (μm)	C/25 capacity (mAh/g)
Low-carbon	0.40	NK[a]	43	10.4	9	10	90	91
LBNL	0.9	700	200	7.3	12.7	8	70	149
MIT	<1	50-100	36	4.4	10	11	55	150
HQ	1-2	200	77	9.2	9	10	85	144
Slovenia	6.1	<100	30	8.9	10	10	85	144
Waterloo	15	100-200	81	7.8	17.2	8	80	130

[a] NK Not known.

model parameters extracted for these two cathodes would be a reflection of not only the materials characteristics, but also the electrode-construction characteristics. However, the LBNL cathode construction recipe is similar to the ones used in this paper; therefore, the impact of electrode construction is expected to be minimal on the results reported here.

The powders were analyzed with XRD to verify phase purity and get an estimate of the average crystallite size by whole pattern fitting. Cathode performance was tested in a half-cell, as discussed above, containing Li reference and counter electrodes, with either 1 M $LiPF_6$ or 1 M $LiBF_4$ in ethylene carbonate/diethyl carbonate electrolyte and Celgard separators. Electrode capacity was determined at a low rate (~C/25), and high-rate utilization was measured at discharge rates from C/5 to 10C (based on a capacity of 170 mAh/g), as controlled with an Arbin Battery Cycler (College Station, TX).

Model Development

The model developed describes the diffusion of lithium and/or electrons in the solid phase and the phase change in the material using the shrinking-core approach, with a core of one phase covering a shell of the other phase, as described previously.[16] The model solves for the diffusion in the shell and the movement of the phase interface by assuming that the concentration at the phase interface is at equilibrium. In addition, the distributed reaction in the porous electrode is described using porous electrode theory, and the change in concentration of the electrolyte is accounted for using concentrated solution theory, as described previously.[15] Two particle sizes are included in the model to approximate the behavior of a true particle size distribution. The carbon coating that is known to exist in this material is not described in the model, and no distinction is made between this carbon and the extra added carbon when electrodes are fabricated. Instead, all conductivity effects are combined into the matrix phase conductivity, whose magnitude is thought to capture the impact of both these carbons.

Note that in the solid iron-phosphate particles, the lithium and the electron are envisioned to form a dilute binary electrolyte. This allows us to collapse the diffusion and migration terms into a single Fick's law-type equation, as shown in Newman.[17] This means that the diffusion coefficient used in this paper is an effective diffusion coefficient which takes the form

$$D = \frac{z_+ u_+ D_- - z_- u_- D_+}{z_+ u_+ - z_- u_-} \quad [1]$$

where z represents the charge on the ion, u the mobility, and D the diffusion coefficient. The subscript + represents the Li ion and the − represents the electron. Using the Nernst-Einstein relationship to relate the mobility to the diffusion coefficient and substituting in the charge of the electron and the lithium ion, Eq. 1 can be rewritten as

$$D = \frac{2D_+D_-}{D_+ + D_-} \quad [2]$$

Therefore, the diffusion coefficient used in this paper depends on the relative magnitude of the electron and lithium-ion diffusion coefficients. Recently, Morgan *et al.* used first-principle calculations to estimate the diffusion coefficient of lithium in $LiFePO_4$ assuming that the concentration and mobility of electrons are large.[18] The authors concluded that the transport of lithium in the lattice is very large (of the order of 10^{-9} cm^2/s), thereby suggesting that electron transport is slower than lithium-ion transport in this material.[18] Using this result in Eq. 2 suggests that the diffusion coefficient used in this paper (8×10^{-18} m^2/s) would be two times the diffusion coefficient of electrons in the $LiFePO_4$ lattice. However, if lithium transport is also equally important when compared to the electron transport, as argued by Yang *et al.*,[19] then, using this result in Eq. 2 suggests that the diffusion coefficient used here is equal to the diffusion coefficient of lithium ions (which is similar to that of the electrons).

We have previously used a well-characterized cell, based on the HQ material, where the particle sizes, area for reaction, loading, and thicknesses were known, to compare the model to the data and extract unknown parameters.[16] This cell was used to estimate the equilibrium potential expression and the composition ranges of the single-phase regions in the material. The diffusion coefficient of electrons in the material was fit using the model to experimental data, resulting in a value of 8×10^{-18} m^2/s, consistent with values reported in the literature. The kinetics was assumed to be large, keeping with the prevalent view that the Li reaction is facile. A value of 3.14×10^{-6} A/m^2 [at a reference concentration of 1 M and 50% state of charge (SOC)] was used for the simulations. These two values were then maintained for all the simulations reported here. All electrolyte properties were the same as those used in Ref. 16 and correspond to $LiPF_6$ salt in either ethylene carbonate (EC):ethylmethyl carbonate or EC:diethyl carbonate. One cathode used in this study (MIT) was cycled in $LiBF_4$ electrolyte, but due to lack of transport properties for this salt, the simulations were conducted using the properties for $LiPF_6$. We have previously shown[16] that electrolyte drops are negligible in cells with thickness and porosities similar to those used in this study. Hence, the electrolyte transport properties used should have little impact on the results presented here.

The comparison of the various materials reported here was performed by first fitting the model to experimental data at various rates to extract the two particle sizes, the matrix conductivity, and the contact resistance, and then using these numbers to simulate behavior for a fixed cell design. Measuring particle sizes using transmission electron microscopy (TEM) can be difficult due to agglomeration effects. In addition, the technique results in a range of sizes, whereas the model requires the use of two characteristic sizes which give the same overall behavior as the real electrode. Finally, the

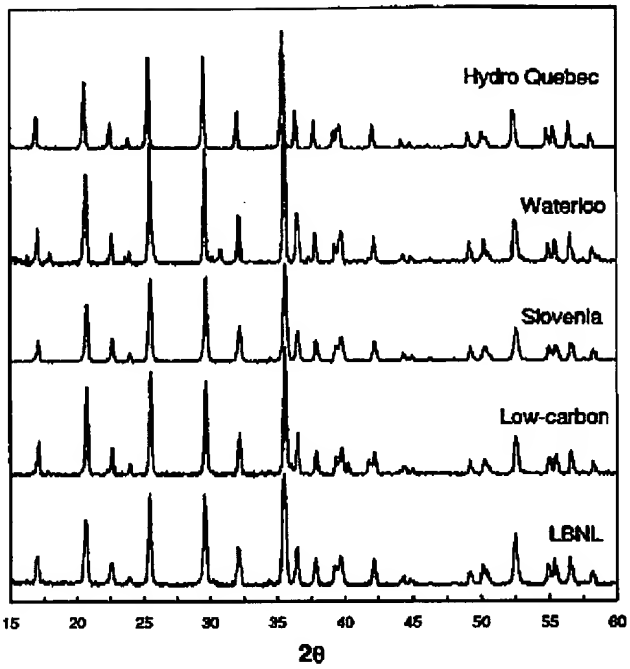

Figure 1. XRD diffraction pattern for five of the $LiFePO_4$ samples used in this study.

surface area measurements based on the Brunauer, Emmett, and Teller method from which particle size can be estimated, can result in areas that can be different from the electrochemical surface area, especially for samples that have a lot of carbon. For these reasons, the particle size was chosen as a fitting parameter. The approach used for incorporating the particle size involves three additional parameters: the sizes of the small, the large, and the average particles. The sizes of the small and large particles dictate the transport losses in the system, and the size of the average particle is needed to find the total surface area of reaction, which in turn affects the kinetic losses. As the exchange current density is taken to be fairly large, the area has little impact on the simulations; therefore, the model can be thought to have two unknown parameters that describe the particle size. We first fit the model to the utilization at the largest current to find the size of the small particle. Subsequently, we fit the utilization at the lowest current to find the size of the large particles. The parameters are then tested by predicting the utilization at other currents. An average value between these two limits was used for the area calculations. As noted earlier, this quantity has little significance to the results shown in the paper. The slope of the potential-capacity curve at intermediate capacity values at the largest current is then used to extract the matrix-phase conductivity. This slope occurs because of a changing reaction distribution in the porous electrode as discharge proceeds. Subsequently, we fit the voltage drop at this current to find the contact resistance between the current collector and the electrode. The contact resistance was negligible for all materials except for the one prepared by the MIT group. These two values are then tested by predicting the voltage and the slope at all other currents. For each material, the C/25 discharge curve was assumed to represent the equilibrium potential in the single-phase region and a curve fit to an equation was used in the model. This data was also used to calculate the maximum capacity of each electrode. Once these parameters are extracted and tested, the comparison of the various materials is performed by simulating their behavior for a single thickness, porosity, and volume fraction of active material.

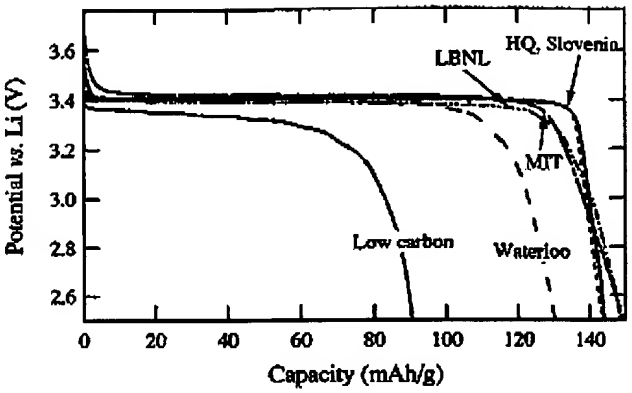

Figure 2. Slow rate (C/25) discharge curves of the six $LiFePO_4$ electrodes vs. Li reference and counter electrodes measured at 25°C.

Results and Discussion

$LiFePO_4$ materials properties.—The samples were received over a period of a year and do not necessarily represent the best $LiFePO_4$ from any of the labs. The low-carbon sample from SUNY was included as a baseline material to show the performance of $LiFePO_4$ with very low carbon content. However, the carbon in this sample was measured to be 0.4% by Luvak Laboratories (Boylston, MA). This amount of carbon resulted from the incomplete combustion of the organic precursors. XRD analysis was carried out for

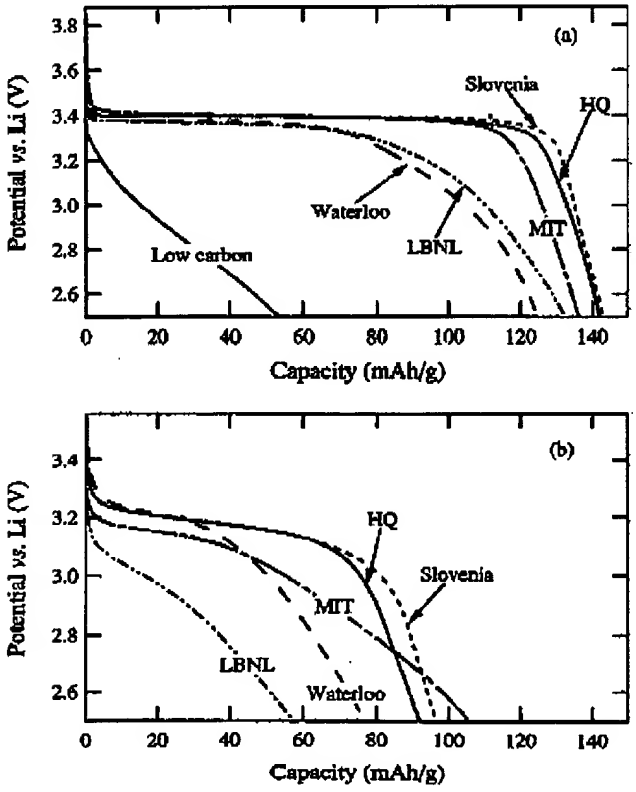

Figure 3. Experimental discharge curves at (a) C/5 and (b) 5C rates for six $LiFePO_4$ electrodes. At 5C the sample with low-carbon coating is not shown as there was no useful capacity in the material.

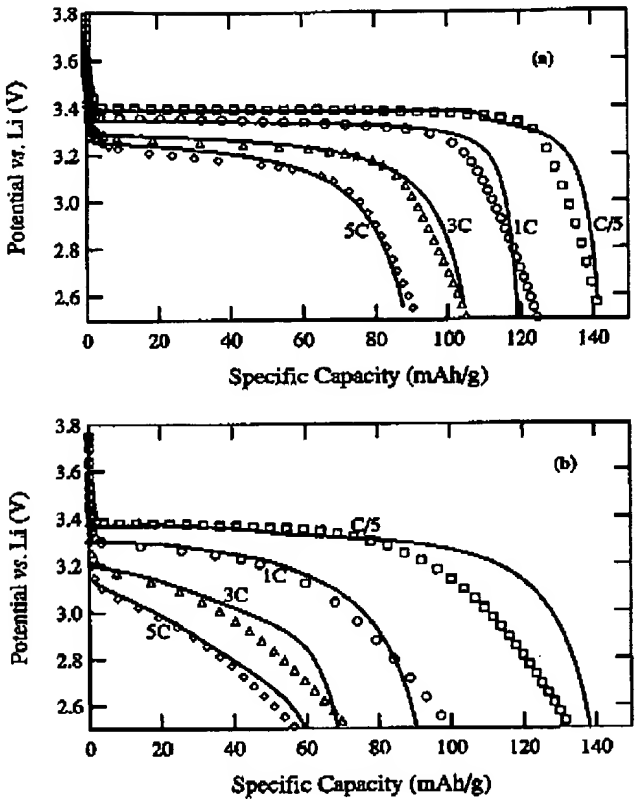

Figure 4. Model-experimental comparisons of discharge curves at various rates for (a) HQ and (b) LBNL material. See text for details.

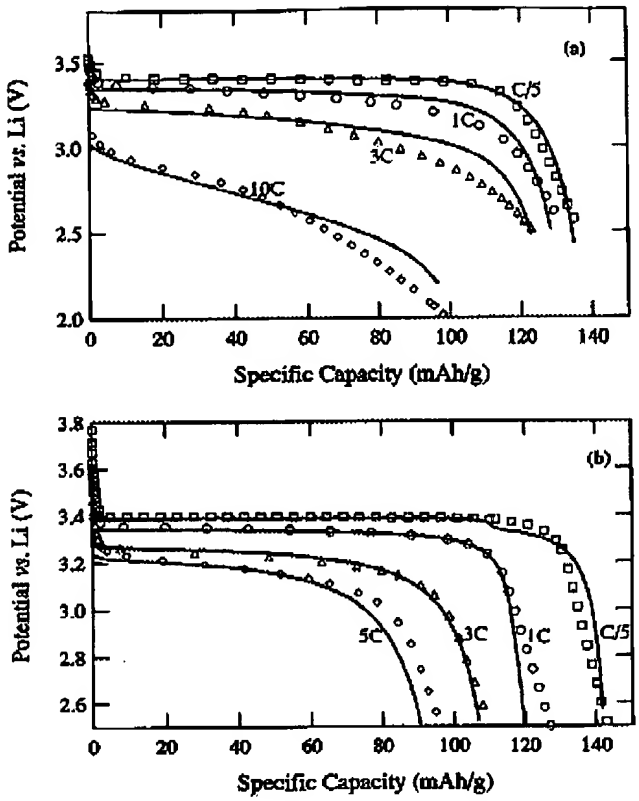

Figure 5. Model-experimental comparisons of discharge curves for (a) MIT and (b) Slovenia material. See text for details.

most of the electrodes, as shown in Fig. 1. Comparison of the powder pattern for all $LiFePO_4$ samples shows that they are well crystallized in the orthorhombic (*Pmnb*) structure of $LiFePO_4$.[20,21] However, some powders show a few very weak reflections from Fe^{3+}-containing impurities such as iron oxide and/or lithiated iron oxide. The weak reflections are mostly due to the low concentration of material in the powders as well as the lower crystallinity. Crystallite sizes were calculated from these diffraction data by whole-pattern fitting. These are summarized in Table I, along with the sources of $LiFePO_4$, the percentage of *in situ* carbon (carbon resulting from the preparation process), and estimates of the primary particle sizes taken from the literature or supplied by the various sources of the $LiFePO_4$ materials. The large variety in particle sizes and particle-size distributions mirrors the wide variety in preparation techniques used for the active materials.

Electrochemical studies.—The compositions and loadings for the different cathodes tested are listed in Table I. The fraction of active material in the cathode matrix fell in the range of 75-82%. It was not possible to keep the total carbon content the same because the Waterloo active-material powder contained 15% carbon and the MIT cathode only 10%, as received. All the cathodes were tested with two cycles at C/25. The second of these discharge cycles is compared in Fig. 2. A specific capacity close to 150 mAh/g was observed for all of the cathodes except for the highest and lowest *in situ* carbon samples (0.4 and 15%), as summarized in Table I. The capacity of the Waterloo material was much lower than reported previously[4] and may hint at a degradation process in this material. Note the differences in the shape of the equilibrium curve at the end of discharge. Whereas the drop in potential is very sharp for the materials prepared by HQ and Slovenia, the other samples show a more gradual drop. Although a C/25 discharge may not be a true thermodynamic measurement, this may indicate differences in the phase composition in these materials.

Our standard protocol for variable-rate measurements uses a constant charge at C/2, so that all the discharges start from the same place and the test can finish in a timely fashion. However, for modeling purposes, it is more convenient to assume that the cathode starts at a fully charged state before each variable-rate discharge. Therefore, except for the MIT cathode, the variable-rate discharge data used for the modeling effort were recorded after a C/25 charge. The curves for the C/5 and 5C discharges for the six $LiFePO_4$ cathodes are compared in Fig. 3a and 3b, respectively. Clearly, some treatment of the $LiFePO_4$, either doping or deliberate *in situ* carbon, is necessary for adequate performance of $LiFePO_4$. This is consistent with the early work with uncoated samples.[11] However, further comparison of these data is difficult, because the best discharge curve (for the MIT cathode) is also for the lowest-loading cathode. For this reason, these data were used for fitting purposes to enable comparisons between electrodes with the same design.

Model fits and predictions.—The model described previously was run for all six sets of cathode discharge data, and the results are presented in Fig. 4-6. Figure 4a shows the model-experimental comparisons for the HQ material. The excellent fits seen in this case are expected considering that this is the baseline used to extract the unknown parameters. The model does not predict the initial sharp drop in potential before the plateau region. We believe that this is caused by a narrow single-phase region in the completely delithiated material. As this single-phase region is not included in the model, no prediction of this behavior is expected. The knee in the low-rate (C/5) curve in Fig. 4a is caused by the two particle sizes in the

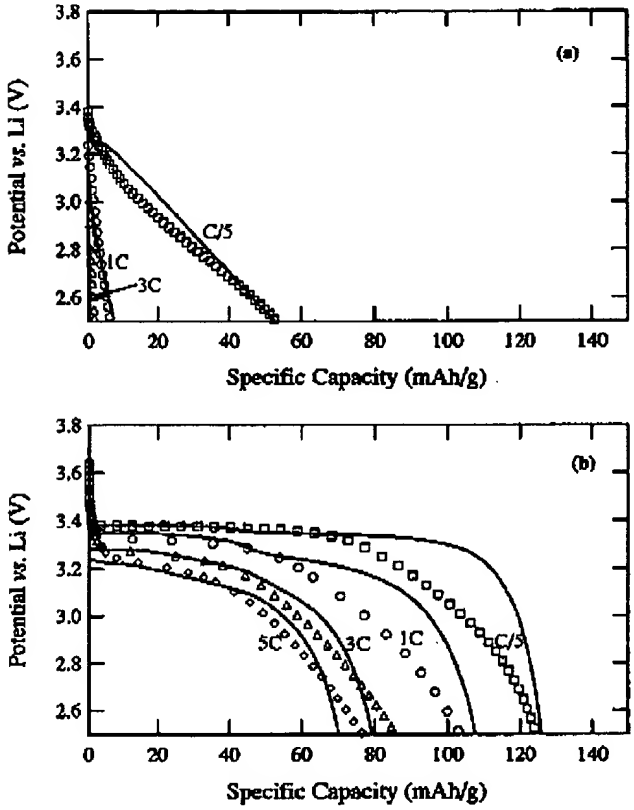

Figure 6. Model-experimental comparisons of discharge curves for (a) low carbon and (b) University of Waterloo material. See text for details.

model. As discharge proceeds, the small particles fill up faster than the larger ones. Typically, this mismatch in the SOC can be expected to result in a greater change in the equilibrium potential of the small particles compared to the large, resulting in a larger overpotential, thereby allowing the larger particles to "catch up." However, the relatively flat potential for this two-phase system does not allow this to occur, and the mismatch between the two particles increases until the small particles are almost completely filled. At this point, the potential drops, and the reaction shifts to the larger particles, resulting in a second plateau. Clearly, incorporating more particle sizes into the model would remove this artifact.

The model predictions for the LBNL material (Fig. 4b) are also excellent, especially in predicting the voltage drops with current. The fit is lacking in predicting the final drop in potential, especially at low rates. The particle sizes extracted for this material had one of the largest ranges among all the materials studied here (see Table II). This suggests that the model needs to incorporate more particle sizes to predict this final decrease in voltage accurately.

Figure 5a shows the predictions for the material from MIT. As mentioned, this material shows a significantly slopey profile at the end of discharge at low rates as compared to the other materials studied. The remarkable utilization of this material is clear in the figure, where the discharge at the 3C rate shows a potential profile that suggests that decreasing the potential cutoff below 2.5 V would have resulted in the material being completely utilized. This material stands out as having the best high-rate utilization. However, as the rate increases, potential drops occur in this material, suggesting that the preparation conditions have not resulted in an optimum matrix conductivity. In addition, this was the only electrode where a contact resistance was needed to get adequate fits to the data. A value of 0.0017 Ω-m^2 fit the data adequately.

Figure 5b shows the comparison for the Slovenia material. Both the behavior of the material and the extracted parameters are comparable to those from the HQ material. Finally, Figure 6a shows the predictions of the material without carbon and Fig. 6b those of the material from the University of Waterloo. The poor utilization of the material without carbon, even at relatively low rates, is due to the voltage reaching the cutoff potential much before any transport limitations become important. As the electrode is ohmically limited, extracting transport-related quantities (particle size) is not possible. The University of Waterloo material shows excellent prediction of the voltage with current, but poor fits in the drop in voltage at the end of discharge, similar to the material from LBNL (Fig. 4b). This material has an even larger size difference between the small and large particles, as predicted by the model. These two materials (Waterloo and LBNL) show a much larger range when compared to the other materials tested here, and this large range correlates with the inability of the model to predict the voltage drops at the end of discharge at low currents. This qualitative correlation gives credence to the assertion that incorporating more particles would give better fits in this region.

Table II summarizes the particles sizes and matrix conductivities extracted using the model for all the materials. Note that this is an indication of the smallest length scale over which diffusion occurs and is therefore different from an agglomerate size, typically reported in the literature. The sizes extracted are of the order of the crystallite size for the various materials (Table II). In some cases (*e.g.*, LBNL), the small particle size extracted is smaller than the crystallite size. This is a consequence of using two sizes to approximate a true distribution. It is clear that the MIT cathode data were fit with the smallest size and smallest range of particle sizes. We believe that this feature is the cause for the excellent behavior of the MIT material. The agreement with their particle-size data (from TEM) is remarkable. The particle sizes for the low-carbon sample are not significant due to the fact that the electrode was so ohmically limited. The fits of the HQ and the Slovenia cathodes were similar, although that for the HQ gave significantly higher matrix conduc-

Table II. Model fits and comparisons.

		Amount of carbon		Parameters from model fit		
					Particle size (nm)	
Source/name	Crystallite size (nm)	Total (%)	*In situ* (%)	Matrix cond. (S/m)	Small	Large
HQ	77	9	1-2	50	61	144
Slovenia	30	10	6.1	0.1	58	137
Waterloo	81	17.2	15	0.03	21	340
LBNL	200	12.7	0.9	0.01	62	608
MIT	36	10	<1	0.01	64	119
Low carbon	43	9	0.4	0.00035	133	288

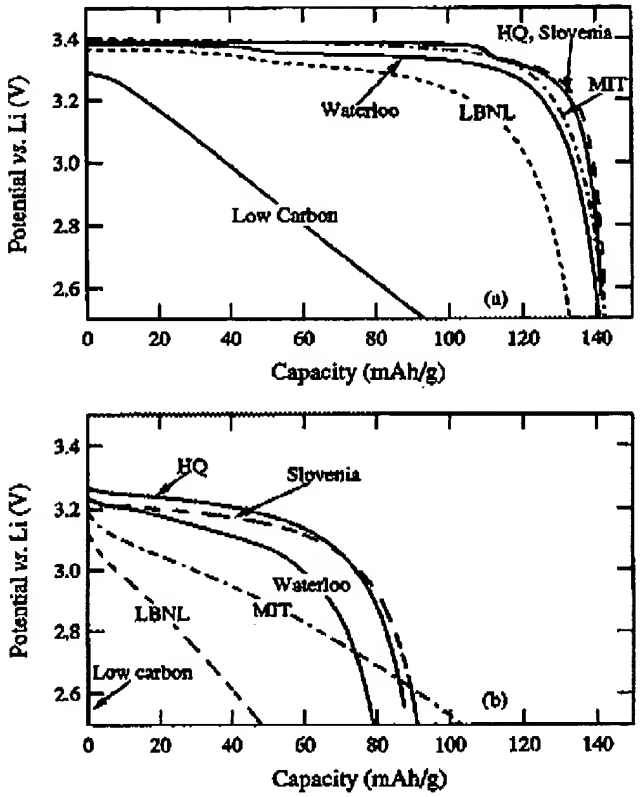

Figure 7. Simulated discharge curves for the six materials used in this study at (a) C/5 and (b) 5C rates. Compare with Fig. 3, which shows results for different designs. Fig. 7 results are for the same design.

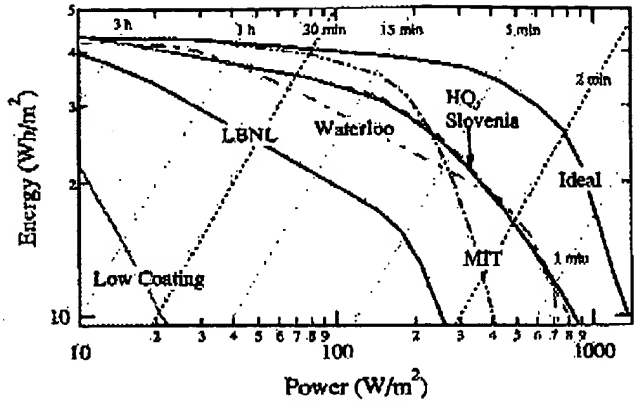

Figure 8. Simulated Ragone plot for the materials studied here. Curves were generated using the parameters extracted from the model-experimental fits, as described in the text, and using these values for a constant cell design. Curve marked Ideal represents a hypothetical cell with particle sizes taken from the MIT material and conductivity of the matrix taken from the HQ material.

tivity. Note that the matrix conductivity value for the HQ electrodes is large enough that ohmic drops are minimal.

The fitting parameters from each source of $LiFePO_4$ were used to calculate the expected performance for a cathode 85 μm thick and with an active material loading of 9.175 mg/cm^2 (the same as the HQ electrode). The calculated C/5 and 5C curves are shown in Fig. 7 and can be compared to the experimental results in Fig. 3. Whereas Fig. 3 shows the experimental data with a different cell design for each material, Fig. 7 shows the simulations for the same cell design. Note that the Waterloo material has almost *ca.* 140 mAh/g in Fig. 7a as the mass of all the materials has been made the same to provide a fair basis for the comparison. In addition, to make the comparison of the MIT material fair, no contact resistance was used in these simulations. The excellent utilization of this material is clearly seen in Fig. 7b, although the potential drops are more significant.

The impact of the decreasing utilization and the drop in potential with current can be captured in one plot by estimating the energy of the cell (area under the voltage-capacity curve) and plotting it against the average power (energy divided by the time of discharge), in the form of a Ragone plot, as shown in Fig. 8. As expected, the electrode with the lowest *in situ* carbon shows the worst performance, while the electrodes from HQ and Slovenia show the best high-rate capability. Although the MIT material shows much better intermediate-rate behavior, a consequence of its smaller particle size, at higher rates, ohmic drops become more important and the energy decreases. The two materials that have the widest particle size range, LBNL and Waterloo, show poor intermediate-rate capability. Of these two, the Waterloo material performs better due to the material's lower average particle size.

Ideal case.—To give the reader an estimate of what can be achieved for this material, we performed a hypothetical simulation by using the best features of these different materials and represent it by the line marked Ideal in Fig. 8. This line was generated by using the particle size of the MIT material and the conductivity of the HQ material. Clearly as much as a doubling of the power capability can be achieved by better material preparation techniques. Each of the materials shown in the figure can be made to achieve this ideal performance, but changes would need to be made to the material properties. In summary, Fig. 8 suggests that for this chemistry to be made more competitive three strategies should be pursued: (*i*) the particle size should be made smaller, (*ii*) the particle size ranges should be minimized, and (*iii*) the matrix conductivity should be improved. Figure 8 also suggests that all three factors are equally important.

However, decreasing the particle size can lead to electrode fabrication issues and could lower the volumetric energy density, caused by the decreasing tap density, as suggested by Chen and Dahn.[22] In addition, smaller particles would require more carbon and binder to bind the particles together to form an electrode, thereby resulting in decreased specific energy. This aspect is beyond the scope of this study; hence, no conclusions can be drawn on an optimum particle size to be used in these electrodes.

Conclusions

Six $LiFePO_4$ electrodes having different particle sizes, carbon contents, porosities, and thickness were examined in this study to understand the mechanism that improves the power capability of this chemistry. This insight is provided by combining experimental data at various rates with a mathematical model. The study suggests that carbon coating is critical as it provides the electron with a more conductive path, thereby decreasing ohmic drops. Although the amount of carbon coating seems immaterial as long as a coating is achieved, the quality of the carbon is important. However, the coating can be eliminated if the active material can be made more conductive, *e.g.*, via doping. However, carbon is still needed to carry the electron from the current collector to the reaction site; therefore, electrode construction can have a significant impact on performance. Finally, the utilization of the material can be poor if the particle size is large, or if the distribution of particle size is wide.

Acknowledgments

We gratefully acknowledge the supply of cathode powders and electrodes from Hydro Quebec, the University of Montreal, MIT, the

University of Waterloo, and the State University of New York at Binghamton. We thank T. Richardson and S. W. Song for the XRD measurements. This research was funded by the Assistant Secretary for Energy Efficiency and Renewable Energy, Office of Freedom-CAR, and Vehicle Technologies of the U.S. Department of Energy under contract no. DE-AC03-76SF00098.

The Lawrence Berkeley National Laboratory assisted in meeting the publication costs of this article.

References

1. N. Terada, T. Yanagi, S. Arai, M. Yoshikawa, K. Ohta, N. Nakajima, and N. Arai, *J. Power Sources*, 1-2, 80 (2001).
2. S.-Y. Chung, J. T. Bloking, and Y.-M. Chiang, *Nat. Mater.*, 2, 123 (2002).
3. N. Ravet, S. Besner, M. Simoneau, A. Vallée, and M. Armand, Hydro-Québec, Can. Pat. 2,270,771.
4. H. Huang, S.-C. Yin, and L. F. Nazar, *Electrochem. Solid-State Lett.*, 4, A170 (2001).
5. S. Yang, Y. Song, P. Y. Zavalij, and M. S. Whittingham, *Electrochem. Commun.*, 4, 239 (2002).
6. S. Y. Chung and Y. M. Chiang, *Electrochem. Solid-State Lett.*, 6, A278 (2003).
7. J. Shim and K. A. Striebel, *J. Power Sources*, 119-121, 955 (2003).
8. K. A. Striebel, A. Guerfi, J. Shim, M. Armand, M. Gauthier, and K. Zaghib, *J. Power Sources*, 119-121, 951 (2003).
9. R. Dominko, M. Gaberscek, J. Drofenik, M. Bele, and J. Jamnik, Abstract 1125, The Electrochemical Society Meeting Abstracts, Paris, France, Vol. 2003-1, April 27-May 2, 2003.
10. J. Barker, M. Y. Saidi, and J. L. Swoyer, *Electrochem. Solid-State Lett.*, 6, A53 (2003).
11. A. K. Padhi, K. S. Najundaswamy, and J. B. Goodenough, *J. Electrochem. Soc.*, 144, 1188 (1997).
12. M. Doeff, Y. Hu, F. McLarnon, and R. Kostecki, *Electrochem. Solid-State Lett.*, 6, A207 (2003).
13. N. Ravet, A. Abouimrane, and M. Armand, *Nat. Mater.*, 2, 702 (2003).
14. L. Nazar, B. Ellis, S. Herle, and O. Crosnier, Abstract 1074, The Electrochemical Society Meeting Abstracts, Paris, France, Vol. 2003-1, April 27-May 2, 2003.
15. M. Doyle, T. F. Fuller, and J. Newman, *J. Electrochem. Soc.*, 140, 1526 (1993).
16. V. Srinivasan and J. Newman, *J. Electrochem. Soc.*, 151, A1530 (2004).
17. J. S. Newman, *Electrochemical Systems*, 2nd ed., Prentice-Hall, Englewood Cliffs, NJ (1991).
18. D. Morgan, A. Van der Ven, and G. Ceder, *Electrochem. Solid-State Lett.*, 7, A30 (2004).
19. S. Yang, Y. Song, P. Y. Zavalij, and M. S. Whittingham, *Electrochem. Commun.*, 4, 239 (2002).
20. A. Streltsov, E. L. Belokoneva, V. G. Tsirelson, and N. K. Hansen, *Acta Crystallogr., Sect. B: Struct. Sci.*, 49, 147 (1993).
21. A. S. Andersson, B. Kalska, L. Häggström, and J. O. Thomas, *Solid State Ionics*, 130, 41 (2000).
22. Z. Chen and J. R. Dahn, *J. Electrochem. Soc.*, 149, A1184 (2002).